

A climate trend analysis of Ethiopia: examining subseasonal climate impacts on crops and pasture conditions

Molly E. Brown¹  • Chris Funk^{2,3} • Diego Pedreros³ •
Diriba Korecha⁴ • Melesse Lemma⁵ • James Rowland² •
Emily Williams³ • James Verdin²

Received: 26 July 2016 / Accepted: 14 March 2017 / Published online: 22 March 2017
© Springer Science+Business Media Dordrecht 2017

Abstract Ethiopia experiences significant climate-induced drought and stress on crop and livestock productivity, contributing to widespread food insecurity. Here, we present subseasonal crop water stress analyses that indicate degrading, growing conditions along Ethiopia's eastern highlands, including productive and populated highland regions. These seasonally shifting areas of increasing water stress stretch from the north to south across eastern Ethiopia, intersecting regions of acute food insecurity and/or high population. Crop model simulations indicate that between 1982 and 2014, parts of eastern Amhara and eastern Oromia experienced increasing water deficits during the critical sowing, flowering, and ripening periods of crop growth. These trends occurred while population in these regions increased by 143% between 2000 and 2015. These areas of enhanced crop water stress in south-central Ethiopia coincide with regions of high population growth and ongoing crop extensification. Conversely, large regions of relatively unpopulated western Ethiopia are becoming wetter. These areas may therefore be good targets for agricultural development.

✉ Molly E. Brown
mbrown52@umd.edu

¹ Department of Geographical Sciences, University of Maryland, College Park, MD, USA

² U.S. Geological Survey, Sioux Falls, SD, USA

³ Climate Hazards Group, University of California, Santa Barbara, Santa Barbara, CA, USA

⁴ Climate Hazards Group, FEWS NET, Nairobi, Kenya

⁵ Ethiopian National Meteorological Agency, Addis Ababa, Ethiopia

1 Introduction

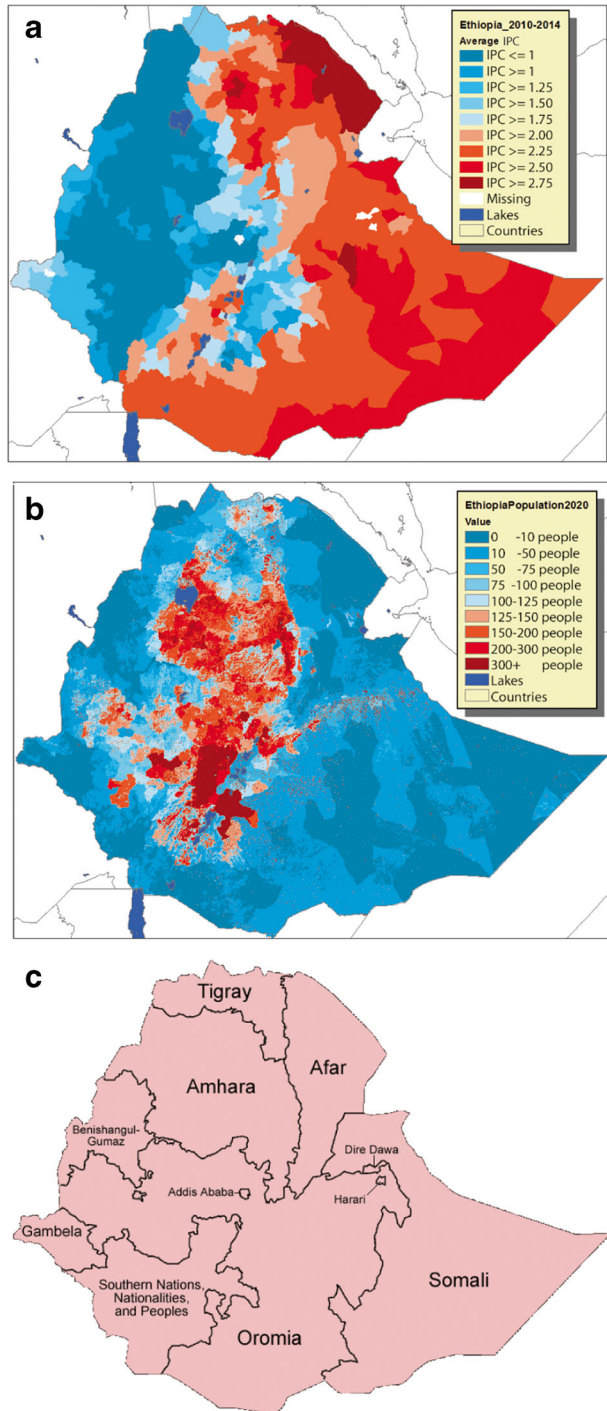
Ethiopia is one of the largest humanitarian aid beneficiaries in the world and experiences significant climate-induced drought and water-related stresses on crop and livestock productivity (WFP 2015). Approximately 95 million people live in Ethiopia, with an expected population doubling time of 23 years (UNDP 2012). Every year, approximately three million Ethiopians are affected by crop production shortfalls, adding to the 7.6 million supported every year by the Productive Safety Net Program (GOE 2015), a social safety net supporting some of Ethiopia's poorest and most food-insecure families.

Like other regions in sub-Saharan Africa, the population structure of Ethiopia is very young, with those under the age of 34 making up one third of the population (UNPD 2012). This demographic structure combined with the low ratio of income earners to consumers makes it difficult to meet the needs for education, health care, and other resources (Williams and Funk 2011). Rapid population growth continues to put pressure on agricultural production, leaving a persistent and growing gap in food availability (Funk and Brown 2009). Despite these challenges, the Ethiopian economy has grown at about 10% or more annually for the past decade, resulting in an increase in the per capita gross national income from \$160 in 2005 to \$470 in 2014 (World Bank 2015). Despite this economic progress, Ethiopia remains one of the most food-insecure countries in the world. Integrated Phase Classification (IPC) provides a consistent means of measuring food insecurity (IPC 2012), and between 2010 and 2014, much of eastern and southeastern Ethiopia exhibited chronic crisis levels of insecurity, with IPC values of 2 or greater (Fig. 1a). Here, we examine recent changes in agricultural water stress in Ethiopia, using a simple crop model, seeking to understand how trends in crop water satisfaction might contribute, or not, to the observed food insecurity.

Agriculture supports more than 85% of the population and constitutes nearly half of the gross domestic product of the Ethiopian economy (CSA 2015). One of the least urbanized countries, Ethiopia depends on wheat (*Triticum* spp.), barley (*Hordeum vulgare*), maize (*Zea mays*), millet (*Panicum* spp.), sorghum (*Sorghum bicolor*), and teff (*Eragrostis tef*) (CSA 2015). Teff, a traditional small grain, is grown by nearly half of all farming households on 28% of all cultivated lands. Teff has become a popular export to the Ethiopia diaspora as well as a cash crop for urban markets. Maize is the second most widely cultivated food crop and is also used for fodder, fencing, and cooking fuel. Most agricultural production is in the regions with the highest rural population densities (Fig. 1b). These regions also have the best market access and the highest probability of having good yields (Chamberlin and Schmidt 2011). Figure 1c also shows Ethiopia's administrative zones.

Previous analyses of Ethiopia rainfall trends have identified March–September rainfall declines across southern and eastern Ethiopia and little change or increasing rainfall over the northwestern parts of the country (Funk et al. 2005; Segele and Lamb 2005; Williams and Funk 2011; Viste et al. 2012; Williams et al. 2012; Jury and Funk 2013). Food security-oriented studies (Funk et al. 2012) describe climate-rainfall interactions that may affect highly populated zones (Funk et al. 2013a). These analyses have identified spring and summer rainfall declines across parts of southern and eastern Ethiopia. The region of Oromia, with more than 11 million people, and Southern Nations, Nationalities, and People's Region (SNNPR), with more than 6 million people, are projected to experience declining rainfall if current trends continue. Funk et al. (2015b) also use a land surface model and Climate Hazards Group InfraRed Precipitation with Station (CHIRPS) data to identify substantial reductions in eastern Ethiopian soil moisture and runoff, and suggest that these reductions arise due to long-term decreases (increases) in rainfall

Fig. 1 **a** Assessment of mean food insecurity levels from 2010 to 2014. **b** The Ethiopian population density per square kilometer in 2020 (*bottom*) from the Famine Early Warning Systems Network (FEWS NET). **c** Map showing the administrative regions of Ethiopia for reference



(air temperatures). These declines across southeastern Ethiopia appear to be related to warming in the Indian Ocean (Funk et al. 2008; Williams et al. 2012) combined with a warming (cooling)

dipole in the western (central) equatorial Pacific (Funk and Hoell 2015b; Funk et al. 2014; Lyon and DeWitt 2012; Williams and Funk 2011). A recovery of boreal summer rainfall in northern Ethiopia (Korecha and Barnston 2007; Viste et al. 2012) appears consistent with the region's positive response to cool east Pacific sea surface (Korecha and Barnston 2007) and a post-1999 tendency for cool east Pacific sea surface temperature conditions (Lyon and DeWitt 2012).

Growing population pressure in these regions means that food demand may outstrip supply unless domestic agricultural yields increase (Funk and Brown 2009). However, the likely changes in agricultural yield vary greatly, given the country's diverse microclimates and cropping patterns (Hurni 1998). Here, we describe trends in rainfall, explore the impact that these changes may have on agriculture, and describe the likely food security consequences of these changes.

2 Data

We use the CHIRPS data to evaluate the variability of Ethiopian rainfall through time (Funk et al. 2015a). The CHIRPS is a 30+-year quasi-global rainfall dataset. Spanning 50° S–50° N and all longitudes, starting in 1981 to 2015, CHIRPS incorporates a 0.05° resolution climatology along with satellite imagery and in situ station data to create gridded rainfall time series for trend analysis and seasonal drought monitoring (Funk et al. 2014b). The CHIRPS dataset has a strong relationship with precipitation datasets such as the Global Precipitation Climatology Center data (Schneider et al. 2008), which is regarded as an accurate estimate of precipitation. The CHIRPS data also incorporates reasonably dense 1981–2014 station data for Ethiopia, obtained from the National Meteorological Agency (NMA). A longer perspective on Ethiopia rainfall is also provided by the new 1900–2014 Centennial Trends precipitation archive for the Greater Horn of Africa (Funk et al. 2016). For context, we also use version 3 of the Gridded Population of the World (GPWv3) (CIESIN 2005). The Gridded Population of the World dataset uses a proportional allocation gridding algorithm using an area weighting method.

GPWv3 was used in this study because it provides homogeneous temporal estimates of observed and projected population at 5-year intervals, based on national census and population registers. The production of spatially explicit disaggregated population grids can generally be achieved using ancillary data, such as nighttime light imagery, roads, and other sources of information, or by the method of proportional allocation, which assumes that population within an administrative unit is solely a function of the area of that unit. GPWv3 follows this latter approach, which produces population maps with less spatial detail, but greater temporal consistency, since ancillary data can change in complex ways. Since we are primarily interested in looking at population at regional scales over multi-year periods, GPWv3 was used in this analysis.

3 Methods

The NMA defines three Ethiopian rainy seasons: the kiremt during June, July, August, and September (JJAS); the belg during March, April, May, and June (MAMJ); and the bega during October, November, December, and January (ONDJ) (NMA 2014). Subseasonal rainfall trends in each of these seasons will have different impacts on pastoral and farming populations. Because rainfed crops require sustained moisture, a reduction in rainfall during the primary growing period, even if the moisture is made up at another time of the year, will reduce crop productivity. Rangelands, however, are less sensitive to the intraseasonal distribution of rainfall.

To describe how observed changes in precipitation translate into impacts on actual crops, we use CHIRPS to drive the water requirement satisfaction index (WRSI). Crop water WRSI is calculated as the ratio of seasonal actual evapotranspiration (AET) to the seasonal crop water requirement (WR). AET is calculated based on the Penman-Monteith potential evapotranspiration (PET) modified by the available soil moisture and crop coefficients to adjust for the growth stages of a crop. The WRSI model is run on a decadal (one third of a month) time step from the onset of rains to the end of the growing period. The onset of rains is triggered when a decadal (one third of a month) receives more than 25 mm of rainfall, and is then followed by two decads with more than 20 mm cumulative rainfall. The growing period is crop specific and varies locally as a function of climatological averages of precipitation and PET. Higher/cooler regions with lower PET have longer growing periods, and these regions can be some of Ethiopia's most productive areas.

The WRSI calculation update each dekad based on the estimated AET and WR. AET varies based on antecedent rainfall, local soil properties, and PET. WR is a crop-specific term that changes over the season based on each crop's phenology. WR increases between onset and the grain filling/flowering crop stages and then decreases through senescence. At each time step, if AET is greater than WR, then AET is set to WR, since there is an upper limit on the amount of moisture the crop can use. When AET is less than WR, the ratio of AET and WR will be less than 1, indicating suboptimal moisture conditions. The seasonal WRSI is then calculated as the cumulative ratio of AET and WR: $WRSI = 100 \times \Sigma(AET) / \Sigma(WR)$, where $\Sigma()$ denotes an accumulation from the onset of rains to the end of the crop growing period.

At the end of the crop growth cycle, the sum of total AET and total WR is used to calculate the proportion of the total potential yield for each growing season. The WRSI at the end of the season is indicative of crop health; values of less than 100 indicate crop water stress. When rainfall deficits do not exist, the WRSI value will be 100, which corresponds to the absence of water-related yield reductions or the attainment of 100% of potential yield for that crop and location. A seasonal WRSI value less than 50 is regarded as a crop failure condition (Smith 1992).

The WRSI is often used in water-limited systems as an indicator of crop performance (Doorenbos and Pruitt 1977; Frere and Popov 1979; Frere and Popov 1986). Here, we use a gridded implementation as in Verdin and Klaver (2002) and Senay and Verdin (2003). The WRSI can quantify the likely cause of changes in the start, end, and length of season, as well as extended intraseasonal dry periods. The Penman-Monteith PET calculation is used because it explicitly incorporates radiation, vapor pressure deficit, and wind impacts. This algorithm has been shown to be generally superior to other algorithms for agricultural applications (Allen et al. 1989) and has been widely used in previous WRSI implementations including Verdin and Klaver (2002) and Senay and Verdin (2003). The advantage of using the Penman-Monteith PET algorithm, as opposed to simpler parameterizations that rely heavily on air temperature, is that it more clearly represents the separate contributions of radiation and near-surface turbulent moisture fluxes, with the latter being strongly controlled by wind speed and vapor pressure deficits (Allen et al. 1989).

In this analysis, we compared WRSI crop production simulations from 1982 to 1998 to the 1999–2014 period. The years 1998 and 1999 were selected as break points based on the known transition in East African climate at that time (Lyon and DeWitt 2012). During each period, the WRSI simulates the emergence and growth of grass, small grains, or maize. Grass requires the least water. Small grains (such as teff or sorghum) require substantially more moisture than grass, and maize requires more water than small grains. We implemented four different season/crop combinations in this analysis: March–November rangeland WRSI

simulations, March–September maize WRSI simulations, May–November grain WRSI simulations, and May–November maize period. For each period, we calculated the difference between the average WRSI from 1982 to 1998 period and the WRSI from 1999 to 2014. This difference highlights the impact of changing rainfall for agricultural production.

We calculated the impact of subseasonal water deficits and visualized the results by presenting standardized plant water deficits from the WRSI model accumulated during the period of flowering and ripening for each crop. Although the WRSI model produces results at each stage of crop growth, we also present the difference between the AET and WR values for the middle of the growing season as these differences reflect the accumulation of water deficits when water stress most acutely affects grain filling. In the flowering and ripening stages of growth, cereals focus on growing grain, not adding leafy biomass. These results are zero if the water needs of the plant are fully met or are less than zero if subseasonal soil moisture deficits stress plant growth. Since these time series follow normal distributions, normal distributions were used to standardize these time series. Means (μ) and standard deviations (σ) are calculated, and standardized z -scores are calculated using the following formula: $z_i = (d_i - \mu)/\sigma$, where i denotes the i th observation. These time series are standardized to facilitate comparisons among crops and regions. This study also uses the Standardized Precipitation Index (Husak et al. 2007) values to represent seasonal rainfall totals. We fit a conditional gamma distribution to each time series and then use the percentile value associated with each precipitation value to derive an equivalent value from a standard normal distribution with a mean of 0 and standard deviation of 1.

4 Results

This analysis shows that there have been reductions in March–June rainfall across central and eastern Ethiopia, with declines ranging from ~ -0.4 to -0.6 Standardized Precipitation Index (SPI) (Fig. 2a). In contrast, northern Ethiopia has seen recent rainfall increases during June–September (Fig. 2b), presumably due to a recent increase in La Niña-like climate conditions.

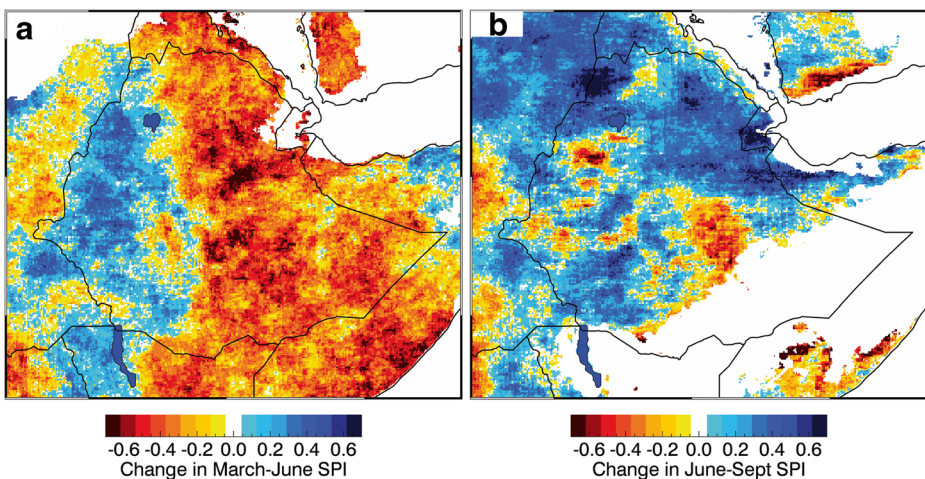


Fig. 2 a March–June and b June–September 1999–2014 changes in standardized seasonal precipitation (SPI) based on the CHIRPS rainfall dataset. Areas with climatological mean rainfall of less than 50 mm have been screened

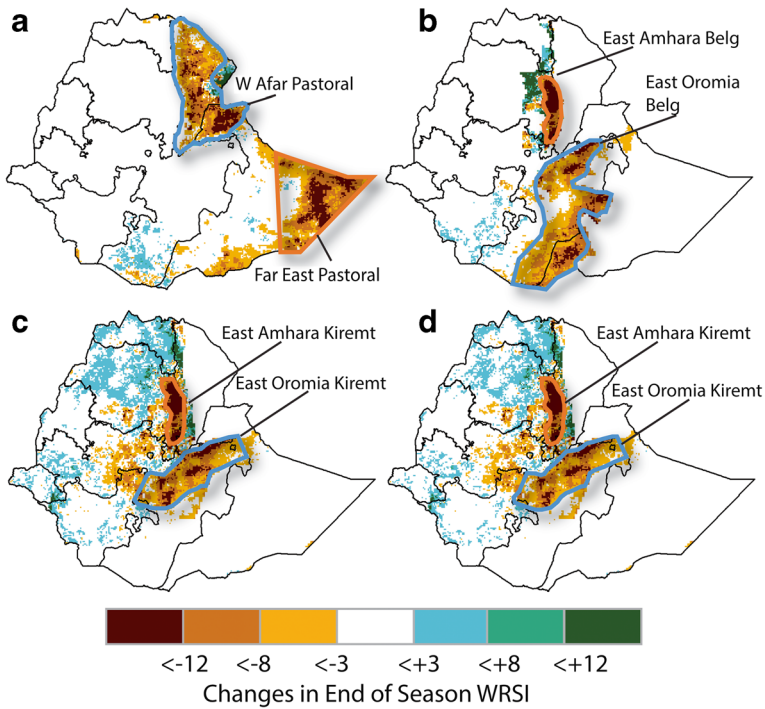


Fig. 3 Analysis of the difference between 1982–1998 and 1999–2014 WRSI seasons. **a** March–November rangeland WRSI simulations. **b** March–September maize WRSI simulations. **c** May–November grain WRSI simulations. **d** More water-demanding May–November maize WRSI simulations

Given the change in sign between these seasonal changes, the WRSI provides an important tool for assessing the relationship between the timing of the rainfall variations and the phenology of crop water requirements.

The difference between the end of season WRSI in the earlier period of 1982–1998 and that in the later period of 1999–2014, when March–June drying began, indicates trends in the success of different growing seasons (Fig. 3). We also see the impact of subseasonal rainfall distribution during the critical periods of flowering and ripening on food production. The impact of water stress can be seen in the maps of WRSI change (Fig. 3a–d). In general, for eastern Ethiopia, the negative effects of March–June rainfall declines (Fig. 2a) tend to overshadow the increases in June–September precipitation (Fig. 2b), leaving the region drier than in previous decades. For pastoral populations, the most affected areas are in the north-eastern part of the country and in eastern Somali Region (Fig. 3a). These areas also are among the most food-insecure areas in the country where population density is increasing (Fig. 1a). A large area of declining WRSI in eastern Oromia and eastern Amhara during March–September is shown in Fig. 3b. Declines along the eastern edge of the growing region in eastern Oromia and eastern Amhara during May–November are shown in Fig. 3c, d. These areas of concern in Oromia and Amhara also have high levels of chronic food insecurity (Fig. 1a).

Figure 4 shows the standardized time series of crop water availability during crop flowering and grain filling, averaged over the hot spot regions shown in Fig. 3a–d. Negative values in these time series indicate poor conditions for successful crop growth. Figure 4a shows that since 1999, about two thirds (9 of 15) of the March–September rangeland seasons in these areas of western

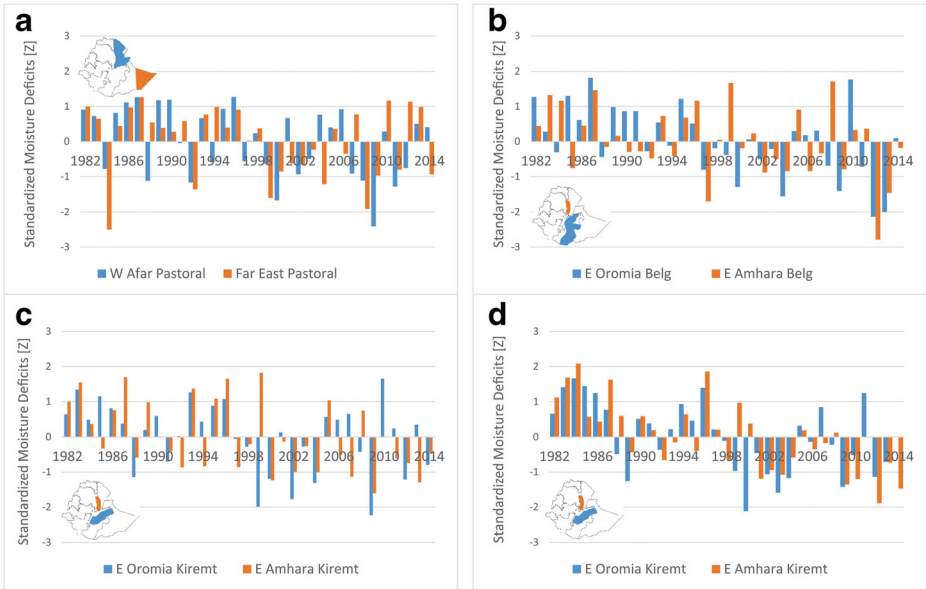


Fig. 4 Time series of standardized subseasonal crop or pasture moisture deficits. Regions noted in **a–d** are highlighted in Fig. 3

Afar and far eastern Ethiopia regions have been below average. During the same period, two thirds (10 of 15) of the March–September maize growing seasons in areas of eastern Oromia and eastern Amhara have been below average (Fig. 4b). For the May–November maize growing seasons, 12 of 15 seasons have been below average; for eastern Oromia May–November grain growing seasons, 9 of 15 seasons have been below average; and for eastern Amhara May–November grain growing seasons, 12 of 15 seasons have been below average (Fig. 4c, d).

We next examine these regional crop water stress conditions using a longer time series of monthly rainfall—the new Centennial Trends precipitation dataset (Funk et al. 2015). While limited station data prevent us from examining submonthly crop model performance directly over a longer time period, we can use gridded monthly data to look further back in time. Figure 5 shows long time series of MAMJ and JJAS precipitation from the Centennial Trends archive (Funk et al. 2015a). The southeastern belg-growing region (associated with the blue time series in Fig. 4b) shows the largest overall decline in MAMJ. Rainfall in this region was plenty in the

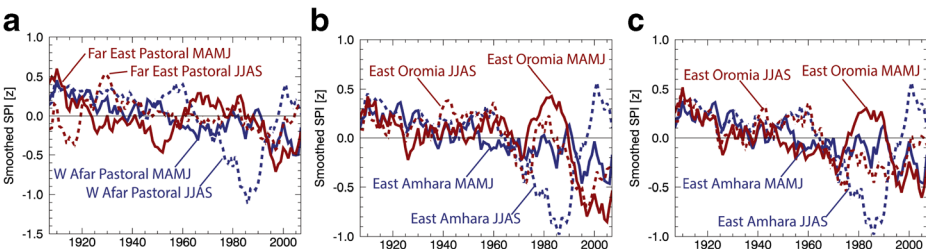


Fig. 5 Standardized Centennial Trends precipitation time series for selected regions. Regions noted in **a–c** are highlighted in Fig. 3. *Solid (dashed) lines* denote MAMJ (JJAS) totals, respectively. All data smoothed with 15-year running averages. **a** Time series from pastoral regions (Fig. 3a). **b** Time series from belg hot spots (Fig. 3b). **c** Time series from kiremt season hot spots (Fig. 3c)

1980s (SPI \sim +0.5) but declined during the 1990s to very low levels (\sim -0.8 SPI), consistent with decadal changes in the gradient between the west Pacific and central Pacific (Funk and Hoell 2015; Funk et al. 2014). The eastern Amhara MAMJ declines also appear substantial compared to 1900–1998 values. In both of these regions, the current MAMJ dryness appears unprecedented in the historical record. Eastern Oromia JJAS rainfall also appears associated with historically low levels during the early twenty-first century. Eastern Amhara rains have a positive relationship to La Niña-like climate, and the area has experienced an increase in rainfall over the 1982–2014 time period. Our WRSI results (Figs. 3 and 4), however, indicate poor subseasonal growing conditions due to the influence of low rainfall during the first half of the growing season.

We conclude this analysis with a brief examination of population change in the target areas. These areas have large and rapidly growing populations that have increased by 180% between 1990 and 2015. The population growth rate of Ethiopia is projected to slow down in the next 35 years. The fertility rate is currently about 4.16 but may reduce to 2.35 by 2050 (CSA 2007). Even with stabilizing the population growth rate, substantially more people would live in Ethiopia, although that growth would be at a slower rate (United Nations 2015). In the Oromia Region alone, the 2050 population may exceed 12 million people. Even without further rainfall declines, Ethiopians likely will be forced to cultivate a limited quantity of land under substantially warming conditions, and that will make expansion into hot lowland areas, which have low agricultural potential, more probable (Ferede et al. 2013). Analysis of land cover changes suggests that this extensification may tend to occur near the densely populated southern half of the country, where forest is being converted into cropland (Funk et al. 2013); in general, transitions from forest to cropland are much more frequent next to villages, and this may support a form of demographic inertia in heavily populated regions (Fig. 1b) of southern Ethiopia, with areas of agricultural expansion coinciding with regions of increased crop water stress (Fig. 3).

5 Discussion

The results of this rainfall and crop model analysis show that Ethiopia has some regions that are likely to be challenged in the coming years. We first discuss the impact of changes in water availability in pastoral regions and then focus on high population density regions that are likely to continue to need international support during anomalously dry growing seasons, even while the Ethiopian economy is diversifying.

5.1 Seasonal trends in rainfall

The reality of climate change in Ethiopia is that some regions are getting wetter, while others are becoming drier (Viste et al. 2012). In Fig. 2, we show the change in SPI (Husak et al. 2008) values, based on CHIRPS data, between 1999–2014 and 1982–1998. During March–June, we find large (greater than half a standard deviation) reductions in rainfall across all of central and eastern Ethiopia, a pattern of drying that extends across much of the Greater Horn of Africa. Figure 2 also shows recent changes in the June–September kiremt rains. Given that rainfall in northern Ethiopia has a negative correlation with the El Niño signal (Korecha and Barnston 2007), we find a recovery in northern Ethiopian rainfall. In eastern Oromia, however, in the densely populated and food-insecure southeastern highlands, we find declines in the SPI for the 1999–2014 JJAS, with 2002 and 2009 regional droughts coinciding with acute food shortages for millions of people.

5.2 Focus on pastoral regions

The direct value of pastoralism in Ethiopia is estimated to be \$1.68 billion per annum, not including the substantial unofficial trade in livestock and livestock products (Nassef and Belayhun 2012). To get these benefits, pastoralists need to produce surplus by maintaining and growing livestock herds and animal body mass. Below-average pasture conditions over multiple years result in poor animal body conditions, low productivity of the sector, and reduced income from the sales of livestock products.

The mobility of herds between areas that have received rainfall is a central part of successful pastoral production. The scattering of different pastures in different places at different times makes pastoralism productive in what is otherwise a difficult environment. Because fresh green pasture does not sprout in the same place at the same time in a region, pastoral families must move herds to long distances to ensure that the herds are fed. Poor pasture resources degrade the health of the herd, reduce household income, and separate women and children from herds and the milk they produce (FEWS NET 2015).

The reductions of rainfall in the Afar and Somali regions have stressed pastoral and agropastoral communities. Livestock is sold to finance purchases of cereals and, in some cases, out of fear of being unable to keep livestock fed and watered until rains start in subsequent growing periods. With multiple below-average growing periods, more livestock is sent to market; consequently, prices depress while cereal demands increase, which further degrades the ability of pastoral communities to meet their caloric needs. Without ongoing food assistance from multiple programs, the poor and very poor households in eastern Afar and Somali regions would be in crisis.

Low belt rainfall for maize and small grains has important consequences in the eastern Oromia and eastern Amhara regions (Figs. 3a–d and 4a–d). Although rainfall continues to be above normal in western regions of Ethiopia (Fig. 2), food prices in the eastern regions continue to be higher than those in other, more developed regions of the country. Rancourt et al. (2014) indicated that beyond poor road quality between major cities, the market structure of the trucking industry and the quality of feeder roads linking villages and the main roads are important contributors to food prices. The cost of transportation consumes more than a quarter of the total price for each animal sent to market from the pastoral zone, reducing the ability of the sector to meet the demands of a growing urban population for meat and milk products (Little et al. 2010). The consequences of ongoing rainfall deficits for pastoral and agropastoral communities in the region may be increasingly unaffordable food prices and degrading livelihoods.

5.3 Impacts of rainfall deficits in high population density regions

Previous analysis identified a pattern of rainfall declines across densely populated, agriculturally important, and vulnerable areas of south-central and southern Ethiopia (Funk et al. 2005). Analysis conducted by Funk et al. (2013) shows the disconnection between where rainfall is increasing and where there are high densities of households reliant on agriculture. The south-central and southern Ethiopian regions, where most of the population is located, have been experiencing declines in rainfall during a 30-year period. Funk et al. (2013) show a land cover analysis that has identified many transitions into cropland in the increasingly semi-arid or arid south that has lower agricultural suitability. In terms of areas with high population, this WRSI analysis has identified the eastern highland areas of Oromia and Amhara as critical hot spots. The Oromia Region has experienced substantial rainfall declines in both MAMJ and JJAS,

while a declining rainfall trend is more pronounced over the eastern sector of the region in MAMJ. This region was also recently analyzed at length (Funk et al. 2015b) using land surface model simulations: both rainfall reductions and warming air temperatures were found to contribute to substantial reductions in runoff and evapotranspiration.

Rainfall deficits and increasing reliance on domestically sourced food have increased the risk of food insecurity. In August 2015, the cost of food in Ethiopia increased to 14.7% from the same month in the previous year. Food price inflation in Ethiopia averaged to 8.2% from 2013 until 2015, reaching an all-time high rate of 14.7% in August 2015 and a low rate of 2.81% in March 2014 (CSA 2015). These price increases challenge farming households' ability to replace grain for consumption when they fail to grow it themselves, because incomes are rarely able to keep up with expenditure needs (Glewwe 1990).

Driven by population pressure, roads, and dense settlement patterns, Ethiopia is becoming more heavily cultivated (Mekasha et al. 2014). The combination of rapid population growth, agricultural extensification, environmental degradation, and decreasing rainfall likely will result in increasing food and water security problems in this region (Pricope et al. 2013; Funk et al. 2013b, 2014a).

5.4 Application of this research in 2015/2016

Here, we briefly document how this research informed effective drought early warning and improved humanitarian assistance during the 2015 Ethiopian food crisis. Analyses such as the one presented here help identify areas experiencing repeated hydrologic shocks. This information can help food security analysts rapidly target severe food crises when the next shock arises. Such was the case in 2015 when rainfall in central and eastern Ethiopia was very poor due to extreme El Niño conditions. The 2015 belg rains were erratic and well below average, and the subsequent June to September kiremt rains started late and were also substantially below average. In combination with extremely warm air temperatures (Funk et al. 2016), the drought resulted in severe water shortages, substantial crop losses, and high levels of livestock mortality. These climatic events were documented in near real time using satellite rainfall estimates from the National Oceanic and Atmospheric Administration (NOAA) and the University of California Santa Barbara (UCSB), vegetation index images from the USGS, and soil moisture anomaly maps derived from land surface modeling by the National Aeronautics and Space Administration (NASA) (FEWS NET 2015). These products clearly identified that in 2015, Ethiopia was experiencing its worst drought in 60 years, with surface water availability reduced by 35% and widespread crop failure.

The Famine Early Warning Systems Network (FEWS NET)'s decision support process enabled the US Agency for International Development (USAID) to make an early and robust response. Following the end of the failed belg season in April 2015, the FEWS NET began providing regular and frequent briefings on the situation to decision makers in Ethiopia and the USA. In August 2015, food assistance totaling 132,570 metric tons had been called forward by the US Agency for International Food For Peace program to support the Government of Ethiopia's Productive Safety Net Program, followed by an additional 154,410 metric tons of food in October 2015 (Wilson 2016). In December 4, 2015, the FEWS NET issued a food security emergency alert that documented the severe 2015 drought, the ongoing food security emergency in the central and eastern parts of the country, and a projection that as many as 15 million people would face severe acute food insecurity requiring assistance in 2016 (FEWS NET 2015). Immediate sustained, large-scale, multi-sectoral emergency assistance to save lives and livelihoods was called for. In

December 11, 2015, the Government of Ethiopia issued a worldwide appeal for over \$1.4 billion in emergency needs to reach over 10 million people, and in February 2016, the USAID deployed a Disaster Assistance Response Team (DART) to Ethiopia to provide technical and relief coordination assistance to the Government of Ethiopia (Wilson 2016).

The USAID stepped up to the challenge, supporting a package of lifesaving humanitarian activities, including food assistance; vital malnutrition treatments; seeds to farmers to begin recovery and to build up depleted food stocks; and emergency water, sanitation, and hygiene assistance. The USAID mobilized nearly \$800 million to support these interventions and, in FY 2016 alone, provided 680,000 metric tons of food assistance to over four million people (FAIS 2016).

6 Conclusions

The World Food Program cites rainfall patterns, land degradation, population density, lack of infrastructure, insecurity and conflict, poverty, and a fall in world prices of cash crops as major threats to food security in Ethiopia. Overall, we found that an analysis of subseasonal crop water stress indicates degrading, growing conditions near the edge of the eastern highlands. Indications of increasing stress are now found in multiple seasons, extending from north to south across the country and intersecting with regions of acute food insecurity, high population density, or both.

In the Afar Region and in the northern and eastern corners of Somali Region, two thirds of the belg seasons have been below average since 1999. This area is home to chronically food-insecure pastoral populations whose economy is dominated by the livestock sector (Sabates-Wheeler et al. 2013; Headey et al. 2014). Warming temperatures due to climate change are likely to affect livestock productivity and health, particularly with growing rainfall deficits affecting the amount of fodder available across large areas (Thornton 2010). In eastern Amhara Region and eastern Oromia Region, two thirds of the belg growing seasons have had water deficits during the flowering and ripening periods of crop growth, thus substantially reducing maize and small grain production. This increasing stress occurred while the populations of these areas increased by 143% between 2000 and 2015, resulting in a sharp increase in the demand for food and the need for cash income to pay for it (Headey et al. 2014).

Changes in rainfall indicate strong seasonal variations, with large declines during MAMJ and some increases in JJAS. Overall, the modeling presented here shows that early season drying in Ethiopia's eastern highland areas reduced food production. Increased crop water stress in south-central Ethiopia corresponds to areas of high population growth and ongoing crop extensification. Conversely, large regions of relatively unpopulated northwestern Ethiopia may be good targets for agricultural development. Better water management strategies and limited mid-season irrigation might also provide strategies for mitigating the impacts of mid-season rainfall deficits in areas currently being farmed.

References

- Allen RG, Jensen ME, Wright JL, Burman RD (1989) Operational estimates of reference evapotranspiration. *Agron J* 81:650–662
- Chamberlin J, Schmidt E (2011) Ethiopian agriculture: a dynamic geographic perspective. IFPRI, Washington DC

- CIESIN (2005) CIAT (Center for International Earth Science Information Network—CIESIN-Columbia University, United Nations Food and Agriculture Programme-FAO, and Centro Internacional de Agricultura Tropical-CIAT): Gridded Population of the World, Version 3 (GPWv3): Po.
- CSA (2015) Ethiopian Agriculture and Natural Resource Statistics. Ethiopian Central Statistical Agency
- CSA (2007) Population and housing census report—country—Ethiopia Central Statistics Agency.
- Doorenbos J, Pruitt WO (1977) Crop water requirements. Food and Agriculture Organization, Rome, Italy
- FAIS (2016) World food aid flows. UN World Food Program
- Ferede T, Ayenew AB, Hanjra MA, Hanjra M (2013) Agroecology matters: impacts of climate change on agriculture and its implications for food security in Ethiopia. *Glob food Secur Emerg issues Econ Implic*:71–112
- FEWS NET (2015) Illustrating the extent and severity of the 2015 Ethiopia drought. Ethiopia Special Report, Washington
- Frere M, Popov GF (1979) Agrometeorological crop monitoring and forecasting. Food and Agriculture Organization, Rome
- Frere M, Popov GF (1986) Early agrometeorological crop yield forecasting. Food and Agriculture Organization, Rome, Italy
- Funk C, Brown ME (2009) Declining global per capital agricultural capacity and warming oceans threaten food security. *Food Secur J* 1:271–289
- Funk C, Harrison L, Shukla S, et al (2016) Assessing the contributions of local and east Pacific warming to the 2015 droughts in Ethiopia and Southern Africa.
- Funk C, Husak G, Michaelsen J et al (2013a) Attribution of 2012 and 2003–12 rainfall deficits in eastern Kenya and southern Somalia. *Bull Am Meteorol Soc* 94:S45–S48
- Funk C, Mahiny AS, Husak G et al (2013b) Blending local scale information for developing agricultural resilience in Ethiopia. *Ref Modul Earth Syst Environ Sci* 2:165–175. doi:10.1016/B978-0-12-384703-4.00234-3
- Funk C, Peterson P, Landsfeld M et al (2015a) The climate hazards infrared precipitation with stations—a new environmental record for monitoring extremes. *Sci Data* 2:150066. doi:10.1038/sdata.2015.66
- Funk C, Rowland J, Eilerts G et al (2012) A climate trend analysis of Ethiopia. US Geological Survey, Boulder
- Funk C, Salmanmahiny A, Husak G (2014a) Large scale environmental assessment and degradation management: the case of food insecurity in Ethiopia. *Environ Resour Res* 2:147–166
- Funk C, Senay G, Asfaw A et al (2005) Recent drought tendencies in Ethiopia and equatorial-subtropical Eastern Africa. Famine Early Warning System Network. USAID, Washington DC
- Funk C, Verdin A, Michaelsen J et al (2015b) A global satellite assisted precipitation climatology. *Earth Syst Sci Data* 8:401–425. doi:10.5194/essdd-8-401-2015
- Funk CC, Dettinger MD, Michaelsen JC et al (2008) The warm ocean dry Africa dipole threatens food insecure Africa, but could be mitigated by agricultural development. *Proc Natl Acad Sci* 105:11081–11086. doi:10.1073/pnas.0708196105
- Funk CC, Peterson PJ, Landsfeld MF et al (2014b) A quasi-global precipitation time series for drought monitoring. US Geological Survey, Reston
- Glewwe P (1990) The measurement of income inequality under inflation. *J Dev Econ* 32:43–67
- GOE (2015) Joint government and humanitarian partners' document. Government of Ethiopia and partners. Addis Ababa, Ethiopia
- Headey D, Taffesse AS, You L (2014) Diversification and development in pastoralist Ethiopia. *World Dev* 56: 200–213
- Hurni H (1998) Agroecological belts of Ethiopia. Explanatory notes on three maps at a scale of 1:1,000,000. Soil conservation research programme.
- Husak GJ, Marshall MT, Michaelsen J et al (2008) Crop area estimation using high and medium resolution satellite imagery in areas with complex topography. *J Geophys Res* 113:D14112. doi:10.1029/2007JD009175
- IPC (2012) Integrated food security phase classification technical manual version 2.0: evidence and standards for better food security decisions. Food and Agriculture Organization (FAO), Rome
- Jury MR, Funk C (2013) Climatic trends over Ethiopia: regional signals and drivers. *Int J Climatol* 33:1924–1935
- Korecha D, Barnston AG (2007) Predictability of June–September rainfall in Ethiopia. *Mon Weather Rev* 135: 628–650
- Little PD, Behnke R, McPeak J, Gebru G (2010) Pastoral economic growth and development policy assessment, Ethiopia. Department for International Development (DfID), London, UK
- Lyon B, DeWitt DG (2012) A recent and abrupt decline in the East African long rains.
- Mekasha A, Gerard B, Tesfaye K et al (2014) Inter-connection between land use/land cover change and herders'/farmers' livestock feed resource management strategies: a case study from three Ethiopian eco-environments. *Agric Ecosyst Environ* 188:150–162

- Nassef M, Belayhun M (2012) Water development in Ethiopia's pastoral areas: a synthesis of existing knowledge and experience. Washington DC
- NMA (2014) Annual climate bulletin for the year 2013. Ethiopian National Meteorological Agency.
- Pricope NG, Husak G, Lopez-Carr D et al (2013) The climate-population nexus in the East African Horn: emerging degradation trends in rangeland and pastoral livelihood zones. *Glob Environ Chang* 23:1525–1541
- Rancourt M-E, Bellavance F, Goentzel J (2014) Market analysis and transportation procurement for food aid in Ethiopia. *Socio Econ Plan Sci* 48:198–219
- Sabates-Wheeler R, Lind J, Hoddinott J (2013) Implementing social protection in agro-pastoralist and pastoralist areas: how local distribution structures moderate PSNP outcomes in Ethiopia. *World Dev* 50:1–12
- Schneider U, Fuchs T, Meyer-Christoffer A (2008) Global precipitation analysis products of the GPCP. Global Precipitation Climatology Centre (GPCC)
- Segele ZT, Lamb PJ (2005) Characterization and variability of Kiremt rainy season over Ethiopia. *Meteorog Atmos Phys* 89:153–180
- Senay GB, Verdin J (2003) Characterization of yield reduction in Ethiopia using a GIS-based crop water balance model. *Can J Remote Sens* 29:687–692
- Smith M (1992) Expert consultation on revision of FAO methodologies for crop water requirements. Food and Agriculture Organization (FAO), Rome
- Thornton PK (2010) Livestock production: recent trends, future prospects. *Philosophical Trans R Soc B* 365: 2853–2867. doi:10.1098/rstb.2010.0134
- UNDP (2012) Africa human development report 2012: towards a food secure future. United Nations Development Programme, Rome
- Verdin J, Klaver R (2002) Grid cell based crop water accounting for the Famine Early Warning System. *Hydrol Process* 16:1617–1630
- Viste E, Korecha D, Sorteberg A (2012) Recent drought and precipitation tendencies in Ethiopia. *Theor Appl Climatol* 112:535–551. doi:10.1007/s00704-012-0746-3
- WFP (2015) Ethiopia overview. World food program, Rome, Italy
- Williams AP, Funk C (2011) A westward extension of the warm pool leads to a westward extension of the Walker circulation, drying Eastern Africa. *Clim Dyn* 37:2417–2435
- Williams AP, Funk C, Michaelsen J et al (2012) Recent summer precipitation trends in the Greater Horn of Africa and the emerging role of Indian Ocean sea surface temperature. *Clim Dyn* 39:2307–2328
- World Bank (2015) Data: the World Bank.